RGS7 and -11 Complexes Accelerate the ON-Bipolar Cell Light Response

Jianmei Zhang,[1,2] *Brett G. Jeffrey,*[2,3] *Catherine W. Morgans,*[4] *Neal S. Burke,*[1] *Tammie L. Haley,*[5] *Robert M. Duvoisin,*[5] *and R. Lane Brown*[1]

Purpose. The retinal ON-bipolar cell (ON-BPC) light response is initiated upon deactivation of the metabotropic glutamate receptor mGluR6 and the G protein Go. G protein-based signaling cascades are typically accelerated by interaction of the G protein α subunit with a member of the regulator of G protein signaling (RGS) protein family. The goal of this study was to determine whether RGS7 and/or -11 serve this function in retinal ON-BPCs.

Methods. Retinas from mice lacking RGS11 ($RGS11^{-/-}$), or with a deletion mutation in RGS7 ($RGS7^{\Delta/\Delta}$), or both, were compared to wild-type (WT) by immunofluorescence confocal microscopy. The retinal light response was measured with the electroretinogram (ERG). The kinetics of simulated light responses from individual rod bipolar cells were recorded by whole-cell patch-clamp electrophysiology.

Results. Levels of the R7 RGS interaction partners, Gβ5 and R9AP, were reduced in the outer plexiform layer of the $RGS11^{-/-}$ and $RGS7^{\Delta/\Delta}$/$RGS11^{-/-}$ mice. ERG recordings demonstrated a delay in the rising phase of the ERG b-wave, larger photopic b-wave amplitudes, and increased scotopic threshold response sensitivity in the $RGS11^{-/-}$ and $RGS7^{\Delta/\Delta}$/$RGS11^{-/-}$ mice. The ERG measured from the $RGS7^{\Delta/\Delta}$ retina was normal. Patch-clamp recordings of chemically simulated light responses of rod BPCs revealed a 25-ms delay in the onset of the ON-BPC response in the $RGS7^{\Delta/\Delta}$/$RGS11^{-/-}$ mouse compared with the WT.

Conclusions. RGS11 plays a role in the deactivation of Gαo, which precedes activation of the depolarizing current in ON-BPCs. RGS7 must also serve a role as changes in $RGS7^{\Delta/\Delta}$/$RGS11^{-/-}$ mice were greater than those in $RGS11^{-/-}$ mice. (*Invest Ophthalmol Vis Sci.* 2010;51:1121–1129) DOI: 10.1167/iovs.09-4163

From the [1]Department of Veterinary and Comparative Anatomy, Pharmacology, and Physiology, Washington State University, Pullman, Washington; the [3]Oregon National Primate Research Center, the [4]Department of Ophthalmology and Casey Eye Institute, and the [5]Department of Physiology and Pharmacology, Oregon Health and Science University, Portland, Oregon.

[2]Contributed equally to the work and therefore should be considered equivalent authors.

Supported by National Institutes of Health Grants EY014700 and EY18625 (CWM), EY09534 (RMD), MH067094 (RLB), and RR000163.

Submitted for publication June 16, 2009; revised August 19, 2009; accepted September 4, 2009.

Disclosure: **J. Zhang**, None; **B.G. Jeffrey**, None; **C.W. Morgans**, None; **N.S. Burke**, None; **T.L. Haley**, None; **R.M. Duvoisin**, None; **R.L. Brown**, None

Corresponding author: R. Lane Brown, Department of Veterinary and Comparative Anatomy, Pharmacology, and Physiology, Washington State University, Stadium Way, Wegner Hall, Pullman, Washington; brownla@vetmed.wsu.edu.

The visual ON pathway, which responds to increases in light intensity, originates at the first retinal synapse between rod and cone photoreceptors and ON-bipolar cells (ON-BPCs). Light stimulation causes photoreceptors to hyperpolarize, thereby reducing the rate of glutamate release into the synaptic cleft. ON-BPCs depolarize in response to the light-induced decrease in synaptic glutamate. This unusual sign-inverting synaptic response is mediated by a metabotropic glutamate receptor, mGluR6,[1] which is negatively coupled to the activation of a TRPM1-containing cation channel via the G protein Go.[2–4] Deactivation of mGluR6 leads to depolarization within 100 ms,[5] allowing this signaling cascade to maintain a high degree of temporal resolution.

The kinetics of most heterotrimeric G protein-based signaling cascades are limited by the rate of GTP hydrolysis by the G protein α subunit. Generally, the response time is shortened by the GTPase accelerating activity provided by regulators of G protein signaling (RGS) proteins.[6] Based on time constraints, RGS activity would seem to be required for the ON-BPC light response, since the intrinsic rate of GTP hydrolysis by Gαo is slow, requiring tens of seconds.[7,8] The situation is similar for phototransduction in the photoreceptor outer segments. In this case, GTP hydrolysis by transducin is accelerated by interaction with RGS9–1, a member of the R7 subfamily of RGS proteins, in conjunction with its obligate binding partner Gβ5. The RGS9–1/Gβ5 complex is tethered to the disc membrane by association with a third protein, R9AP.[9] Rods from transgenic mice lacking RGS9–1,[10] Gβ5,[11] or R9AP[12] show normal activation of the photoresponse, but a profoundly slowed time course of deactivation.

RGS9 is one member of a large family of more than 30 RGS proteins.[13] The defining structural element of an RGS protein is the RGS domain, a conserved ~120 amino acid sequence, through which it interacts with Gα subunits to stimulate GTP hydrolysis.[14] RGS proteins in the R7 subfamily, which includes RGS6, -7, -9, and -11,[15] are characterized by a G protein γ subunit-like (GGL) domain, which facilitates interaction with a unique G protein beta subunit, Gβ5. The R7 RGS proteins also contain a disheveled/EGL-10/pleckstrin homology (DEP) domain through which they can bind to G protein-coupled receptors,[16] as well as the membrane-anchoring proteins, R7BP and R9AP.[9,17–20] We and others have previously identified two RGS proteins of the R7 subfamily, RGS7 and -11, that colocalize with mGluR6 in the tips of ON-BPC dendrites,[21–24] where they are poised to play a role in the mGluR6-based signaling pathway.

In this study, we investigated the role of RGS7 and -11 complexes in the mGluR6 signal transduction pathway in mouse ON-BPCs. We compared ON-BPC responses between wild-type (WT) mice and genetically modified mice lacking RGS11 ($RGS11^{-/-}$), or with a deletion mutation in RGS7 ($RGS7^{\Delta/\Delta}$), or both. The targeted mutation in RGS7 is a deletion of exon 11, which encodes 33 amino acids spanning an interdomain region of unknown function and the first 9 amino acids

of the GGL domain.[25] The functionality of this deletion mutant remains to be determined. We report that the absence of RGS11 results in a delayed onset of ON-BPC light responses and increased photopic amplitudes compared with WT mice. The RGS7 deletion alone has no measurable effect on the ON-BPC responses, but it enhances the effect of the lack of RGS11 in $RGS7^{\Delta/\Delta}$/$RGS11^{-/-}$ double-mutant mice.

Materials and Methods

Animals

Heterozygote $RGS7^{+/\Delta}$ ($RGS7^{tm1Lex}$, MGI:3528964; http://www.informatics.jax.org/external/ko/data/Lexicon/8/lexjac1.lexgen.com_3a8080/nih/analysis/imageviewer.jsf@assayid=48&imageid=1606&type=image.htm) and $RGS11^{+/-}$ ($RGS11^{tm1Lex}$, MGI:3528953) mice were originally produced by Lexicon Pharmaceuticals (The Woodlands, TX). $RGS7^{+/\Delta}$ heterozygotes were kindly provided by Theodore Wensel (Baylor College of Medicine, Houston, TX) and $RGS11^{+/-}$ mice were obtained from the Mutant Mouse Regional Resource Center (University of North Carolina, Chapel Hill, NC) purchased from the Texas Institute for Genomic Medicine (Houston, TX). The genetic background of both mutants includes 129S5/SvEvBrd and C56BL6/J. All mice used in this study were from the same breeding colony and share common ancestry. $RGS7^{\Delta/\Delta}$, $RGS11^{-/-}$, double-mutant $RGS7^{\Delta/\Delta}$/$RGS11^{-/-}$, and WT mice were produced by breeding mice generated from $RGS7^{+/\Delta}$ and $RGS11^{+/-}$ heterozygous parents. The WT and homozygous knockout experimental animals were littermates from heterozygous matings. Genotyping was performed as recommended by Lexicon Pharmaceuticals. Animals aged from P21 to P50 were used in this study. All animal procedures were conducted in accordance with the ARVO Statement for the Use of Animals in Ophthalmic and Vision Research and the National Institutes of Health guidelines and were approved by the institutional animal care and use committees at both WSU (Washington State University) and OHSU (Oregon Health & Sciences University).

Immunohistochemistry

Immunohistochemistry on retina sections was performed as described previously.[26,27] Antibodies directed against RGS7, RGS11, Gβ5, and R9AP were kind gifts of Theodore G. Wensel and have been described in the retina.[21] Rabbit polyclonal antibody (R4612) against full-length bovine RGS7 and goat polyclonal antibody against Gβ5 (peptide MATDGLHENETLASLKC) were generated at Bethyl Laboratories (Montgomery, TX). The RGS11 antibody was raised in rabbits against a recombinant polypeptide corresponding to residues 248-471 of mouse RGS11.[28] Antibodies were used at the following concentrations: anti-Gβ5, 1:500–1:1000; anti-RGS7, 1:500–1:1000; anti-RGS11, 1:1000–1:5000; anti-mGluR6,[29] 1:100; and mouse monoclonal anti-PKCα (Sigma, St Louis, MO), 1:5000. Appropriate secondary antibodies were coupled to either Alexa-488, or Alexa-594 (Molecular Probes, Eugene, OR) and diluted 1:2000.

Western Blot Analysis

Retinal extracts containing 10 μg of total protein were subjected to electrophoresis on precast 4% to 12% polyacrylamide gradient gels (Novex; Invitrogen, Carlsbad, CA). The separated proteins were electrophoretically transferred to PVDF membranes, which were probed with different antibodies, as previously described.[29] Secondary antibodies conjugated to IR dyes were used at a dilution of 1:10,000, and visualized with an infrared imaging system (Odyssey; Li-Cor, Lincoln, NE).

In Vitro Electrophysiology

Animals were anesthetized with isoflurane (Halocarbon Laboratories, River Edge, NJ), and subsequently euthanatized by cervical dislocation. For electrophysiological studies, the eyes were enucleated, the anterior segment and vitreous removed, and the posterior eye cups placed in oxygenated Ames medium at 25°C. The retina was isolated, mounted ganglion cell side down on an 0.8-μm cellulose membrane filter (Millipore, Bedford, MA), and vertically sliced (~200 μm) using a custom-made tissue slicer, as described previously.[5] Nitrocellulose strips holding retinal slices were immobilized between two beads of silicone grease on a coverslip and then placed in the recording chamber, which was perfused at a rate of ~2 mL/min with bicarbonate-buffered Ames medium continuously bubbled with 95% O_2-5% CO_2. All procedures were performed under normal visible-light illumination. For ON-BPC recordings, the chamber was heated to 32°C to 34°C, and the medium was supplemented with 4 μM L-aminophosphonobutyric acid (L-AP4; Tocris Bioscience, Ellisville, MO) to maximally activate the mGluR6 receptors, thereby mimicking darkness. Slices were viewed with an upright microscope (BX 51WI; Olympus, Tokyo, Japan) fitted with a ×40 water-immersion objective and infrared gradient contrast optics.[30]

Patch electrodes were fabricated from thick-walled borosilicate glass to have a resistance of 6 to 10 MΩ. For most experiments, the patch electrode was filled with an intracellular solution containing (in mM): 135 K^+-methanesulfonate, 6 KCl, 2 Na_2-ATP, 1 Na-GTP, 1 EGTA, 2 $MgCl_2$, and 5 Na-HEPES (pH 7.4). To slow response run-down in the GTP-γ-S experiments described in Figure 1, the pipette solution contained (in mM): 108 K^+-gluconate, 20 TEA, 10 HEPES, 20 BAPTA, 4 MgATP, and 1 NaGTP, adjusted to pH 7.4 with KOH. Alexa-488 hydrazide (Molecular Probes) was added at a concentration of 100 μM for morphologic identification of bipolar cell types after patch-clamp recording. All chemicals were obtained from Sigma-Aldrich unless otherwise stated.

Whole-cell voltage-clamp recordings were performed at a holding potential of −60 mV with a patch-clamp amplifier (EPC-10; HEKA Instruments, Inc., Bellmore, NY). Chemically simulated BPC light responses were elicited by pressure application of the mGluR6 antagonist, (RS)-α-cyclopropy1–4-phosphonophenylglycine (CPPG; 500 μM; Tocris Bioscience). Pulses were delivered via a 5 MΩ patch pipette onto bipolar cell dendrites for 5 seconds at ~6 psi with a pressure ejection system (Spritzer II; Toohey Instruments, Fairfield, NJ). Current responses were digitally sampled at 20 kHz and filtered at 5 kHz. The amplitude and kinetics of the agonist-induced responses were characterized by measuring three parameters: the time lag between CPPG application and when the response reached 10% of maximum; the 10% to 90% increase-time of the response, and the peak amplitude.

Electroretinogram Recording

ERGs were recorded from 15 WT, 7 $RGS7^{\Delta/\Delta}$, 6 $RGS11^{-/-}$, and 6 $RGS7^{\Delta/\Delta}$/$RGS11^{-/-}$ mice. The mice were dark-adapted overnight (>12 hours), prepared for recording under dim red light, and anesthetized with an intraperitoneal injection of ketamine and xylazine (100:10 mg/kg). Anesthesia was maintained with the same drugs (30:3 mg/kg) delivered approximately every 30 minutes, via a small butterfly infusion needle placed in the flank. Rectal temperature was maintained at 36.5°C to 38°C by placing the mouse on a circulating-water heating pad. A wire loop placed under the upper teeth was used to draw the mouse into a custom-made holder that stabilized the head and allowed delivery of O_2, both of which minimized breathing artifacts during recording. Before ERG recording, the pupils were dilated with 2.5% phenylephrine and 1% tropicamide, and the cornea anesthetized with 1.0% proparacaine. The ERG was recorded from a custom-made contact lens electrode placed against the cornea with a small drop of 1% methylcellulose. A platinum loop placed over the eye and positioned behind the equator served as the reference, and a needle electrode placed in the tail served as the ground.

Flash stimulation was provided by a photostimulator (model PS22; Grass-Telefactor, West Warwick, RI), and two high-intensity photoflash units (a 2405CX and a modified 1205CX power supply with 205 flash units; Speedotron, Chicago, IL), which were mounted at the head of a light tunnel connected to a Ganzfeld. Flash intensity measurements in

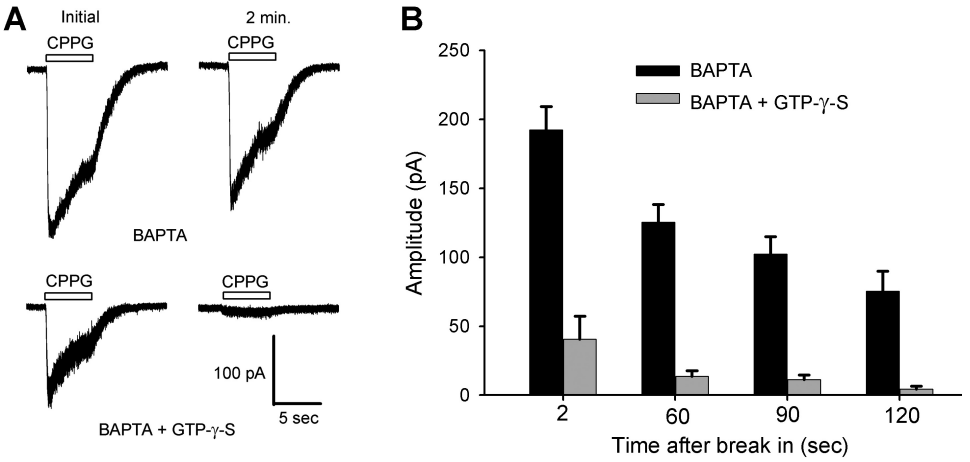

FIGURE 1. GTP hydrolysis is necessary for the activation of the depolarizing light response in ON-BPCs. (**A**) CPPG-activated currents were measured in rod bipolar cells in retinal slice preparations immediately after break-in and at 30-second intervals thereafter. Currents were recorded from rod BPCs in whole-cell voltage clamp mode at a holding potential of −60 mV. The retinal slice preparation was bathed in the mGluR6 activator, L-AP4 (4 μM), to simulate darkness, and a 5-second puff of the inhibitor CPPG (500 μM) was applied to the dendritic terminals to simulate light stimulation. The pipette solution contained a high concentration of BAPTA to delay current decline. For the traces labeled GTPγS, the pipette solution also contained 300 μM GTPγS. (**B**) Summary of CPPG-induced current magnitude with control pipette solution and GTPγS-containing internal solution (control traces, $n = 13$; GTPγS traces, $n = 8$; error bars, SEM).

candela-s/square meter were made with an optometer (350 linear/log optometer; UDT Instruments, San Diego, CA) set to integration mode. Scotopic conversions were estimated based on the color temperatures of the flash units.[31]

Full-field scotopic ERGs were recorded to flashes of increasing intensity (−6.4 to 2.4 log scotopic [scot] cd-s/m^2). The interval between flashes ranged from 2 to 150 seconds for the dimmest to highest intensities. ERGs were the averages of 5 to 60 responses for flash intensities < −3.2 log scot cd-s/m^2; for higher intensities, ERGs were recorded to a single/paired flash. Rod-isolated ERGs were obtained by subtracting dark-adapted cone-isolated ERGs from the mixed rod/cone responses for flash intensities above −1.0 log scot cd-s/m^2. Cone ERGs were obtained with a paired flash protocol; the first flash saturated the rods for a defined interval, during which a second flash produced an isolated cone response.[32,33] For flash intensities below 1.5-log scot cd-s/m^2, each flash was presented 0.7 second after a 1.6-log scot cd-s/m^2 conditioning flash. At higher intensities, identical paired flashes were separated by 0.7 to 1.5 seconds. Full-field photopic ERGs were recorded in response to flashes of increasing intensity (−1.4 to 3.7 log phot cd-s/m^2) presented against a rod-saturating background (60 cd/m^2). Photopic ERGs were the averages of 2 to 60 responses.

Scotopic threshold responses (STRs) generated in the proximal retina were recorded by low-pass filtering the ERGs at 30 Hz (−3 dB) for intensities up to −3.9 log scot cd-s/m^2. For higher intensities, the low-pass filter was set to 300 or 1000 Hz for intensities lower or higher than −0.4 log scot cd-s/m^2, respectively. All ERGs were amplified (2–10 K) and high-pass filtered (−3 dB at 0.1 Hz) before being sampled at 5 kHz with a 12-bit A/D converter and stored for off-line analysis. Total recording time, including setup, was typically 1.5 hours.

ERG Analysis

To study the kinetics of the rising phase of the ERG response, we calculated the rate of increase from the derivative of the filtered ERG (i.e., dERG(t)/dt) after digital isolation and subtraction of the oscillatory potentials. The oscillatory potentials (OPs) were digitally isolated with an anticausal, Chebychev filter (−3 dB at 30 and 300 Hz), using routines written by the authors in commercial software (MatLab; The MathWorks, Natick, MA). The lower cutoff of the band-pass filter was set at 30 Hz since this frequency enabled isolation of all OPs, even for the highest flash intensity, but did not introduce distortion into the rising phase of the ERG response (see Fig. 5B). The rates of increase were calculated for all photopic recordings and for scotopic ERG b-waves recorded to flash intensities below −1.5 log scot cd-s/m^2 before intrusion of the a-wave. Maximum rate of increase was obtained from the peak of the derivative.

To quantify rod photoreceptor kinetics, a P3 model was ensemble fitted to the leading edges of bright flash ERG a-waves.[32] The derived parameters were: S [(sc cd-s/m^2)$^{-1}$ s^{-2}], the rod sensitivity parameter that scales flash intensity; t_d (in milliseconds), the delay due to the filter and finite duration of the flash; and $R\text{max}_{P3}$ (in microvolts), the maximum rod response. The changes in the ERG b-wave were quantified by fitting a Naka-Rushton function to the plot of the ERG b-wave amplitude against flash intensity.[34] Only b-waves recorded to flash intensities above −4.0 log scot cd-s/m^2 were included in the fit, to avoid any significant STR contributions from the proximal retina. The derived parameters were the response maximum, V_{max} (in microvolts), and the flash intensity that produces the half-maximum response, K (scotopic candela-seconds/square meter). One-way ANOVA was used for ERG parameters. For analyses that indicated a significant effect, post hoc tests were performed with Bonferroni correction for multiple comparisons. For all comparisons, the level of statistical significance was set at $P < 0.05$ before Bonferroni correction.

RESULTS

Requirement for GTP Hydrolysis for Activation of the Depolarizing Light Response in Rod Bipolar Cells

Whole-cell patch-clamp recordings were obtained from rod BPCs in slices of mouse retina. The dark state was mimicked by bathing the slices continuously in a saturating concentration (4 μM) of the group III mGluR agonist, L-AP-4. This treatment activates the mGluR6 cascade, resulting in closure of the transduction channel and hyperpolarization of the cell, as would occur when glutamate is released by photoreceptors in the dark. Responses were elicited by puffs of 500 μM CPPG, an antagonist of group III metabotropic glutamate receptors. CPPG application simulates the light-induced decrease in synaptic glutamate, displacing L-AP4, and thereby opening the mGluR6-coupled transduction channel. A concentration of 500 μM CPPG is sufficient to fully antagonize bath L-AP-4 and turn on the maximum transduction current. The overall shape of chemically simulated light responses (Fig. 1A) is similar to that of true light responses.[5]

Rod BPCs begin to depolarize within 100 ms in response to the light-induced decrease in synaptic glutamate levels.[5] This depolarization is thought to be mediated by deactivation of mGluR6 and the G protein, Go, which requires rapid hydrolysis of the bound GTP. To verify this fundamental underlying assumption about the mGluR6-based signaling cascade in mouse ON-BPCs, we performed recordings in which the nonhydrolyzable GTP analogue, GTP-γ-S, was included in the intracellular electrode solution. The intracellular solution also contained a

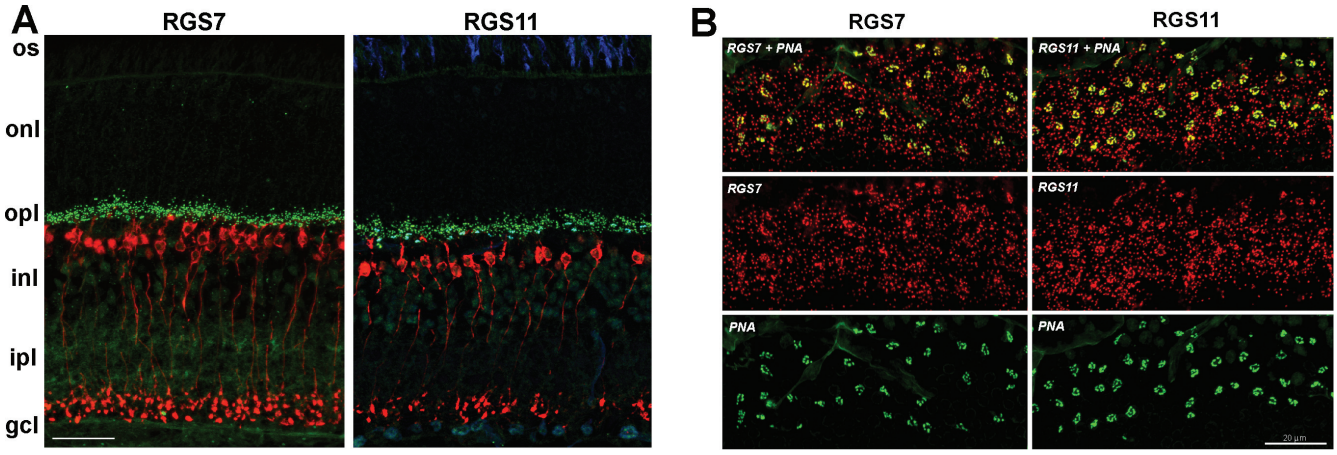

FIGURE 2. RGS7 and -11 are associated with both rod and cone ON-BPCs. (**A**) Labeling of a mouse retinal section for RGS7 (*green*, *left*) and the rod-BPC marker, PKCα (*red*). Triple labeling for RGS11 (*green*, *right*), PKCα (*red*), and the cone marker, peanut agglutinin (PNA, *blue*). Scale bar, 20 μm. (**B**) Oblique retina sections through the OPL were double labeled for PNA-Alexa488 (*green*) to mark cone pedicles and either RGS7 (*left*) or RGS11 (*right; both red*). In the merged image, co-localization of PNA and the RGS proteins to cone terminals appears *yellow*. The *red* puncta in the merged image are associated with rod terminals.

high concentration of the calcium chelator, BAPTA, which has been shown to eliminate the rapid current decline in rod bipolar cells and dramatically reduce time-dependent rundown of the light-activated current.[35] In control cells containing BAPTA, the CPPG-activated current declined by ~50% over a 2-minute interval (Fig. 1A). In contrast, if the electrode was filled with a solution containing GTP-γ-S, the initial CPPG-activated current (recorded immediately after break-in) was reduced by ~75% and decayed rapidly over time. After a 2-minute interval in the presence of GTP-γ-S, the CPPG-activated current was reduced to 5% of its original value (Fig. 1B). Similar to previously reported results,[36,37] these experiments demonstrate that GTP hydrolysis is necessary to elicit the depolarizing current in ON-BPCs.

Association of RGS7 and -11 with Rod and Cone Terminals in the OPL

We have shown that Gβ5 is localized to the OPL of the retina, where it co-localizes with mGluR6.[21] Of the family of R7 RGS proteins (RGS6, -7, -9, and -11) that are known to bind Gβ5, RGS7 and -11 are present in the OPL (Fig. 2A), where they form a complex with Gβ5.[21] To determine whether RGS7 and -11 are differentially distributed between rod BPCs and cone ON-BPCs, we double-labeled obliquely cut OPL sections for either RGS7 or -11, and the cone photoreceptor marker, peanut agglutinin (PNA). The results in Figure 2B indicate that both RGS7 and -11 complexes are associated with cone pedicles as well as rod spherules, supporting the conclusion that rod BPCs and cone ON-BPCs contain both RGS7 and -11 complexes.

Effect of the RGS7 and -11 Mutations on Other ON-BPC Proteins

To examine the effect of RGS7 and -11 on the expression of other ON-BPC proteins, we compared protein levels and distribution of Gβ5, RGS7, RGS11, and R9AP in retinas from WT, $RGS7^{\Delta/\Delta}$, $RGS11^{-/-}$, and $RGS7^{\Delta/\Delta}/RGS11^{-/-}$ mice. RGS11 was undetectable in both the $RGS11^{-/-}$ and $RGS7^{\Delta/\Delta}/RGS11^{-/-}$ retinas by both immunoblot analysis of retinal extracts and immunofluorescent staining of retina sections (Figs. 3). There was little difference in RGS7 immunofluorescence in the OPL of the different mouse genotypes; however, on immunoblots the apparent molecular weight of two RGS7 immunoreactive bands was each reduced by ~4 kDa in the $RGS7^{\Delta/\Delta}$ and $RGS7^{\Delta/\Delta}/RGS11^{-/-}$ lanes, consistent with the predicted loss of

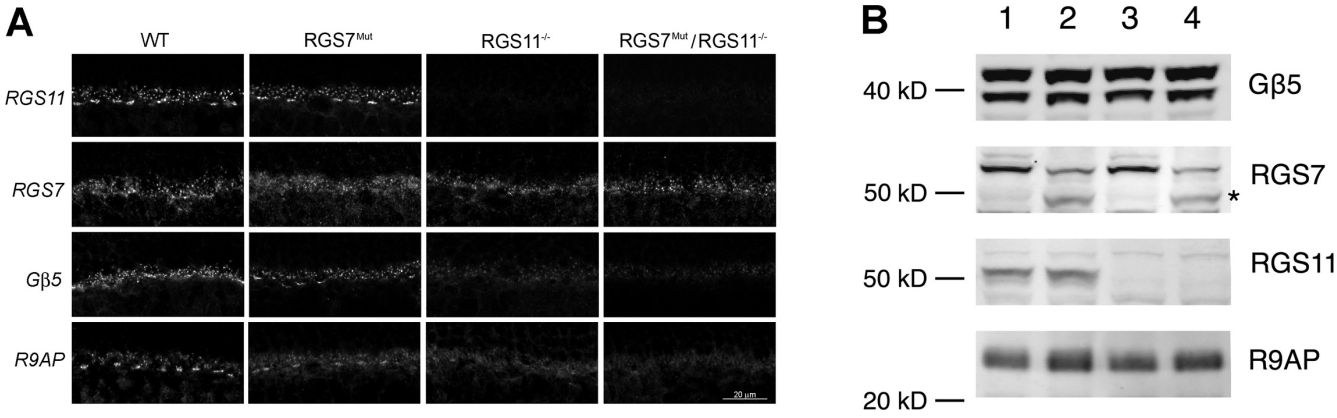

FIGURE 3. Levels of RGS7, RGS11, and associated proteins are altered in the OPL of RGS mutant mice. (**A**) Immunofluorescent labeling for RGS7, RGS11, R9AP, and Gβ5 in the OPL of WT, $RGS7^{\Delta/\Delta}$, $RGS11^{-/-}$, and $RGS7^{\Delta/\Delta}/RGS11^{-/-}$ mice. (**B**) Western blot analysis of total retinal protein from WT (*lane* 1), $RGS7^{\Delta/\Delta}$ (*lane* 2), $RGS11^{-/-}$ (*lane* 3), and $RGS7^{\Delta/\Delta}/RGS11^{-/-}$ (*lane* 4) mice probed for RGS7, RGS11, R9AP, and Gβ5. (⋆) The major RGS7 band in the RGS7 deletion mutant.

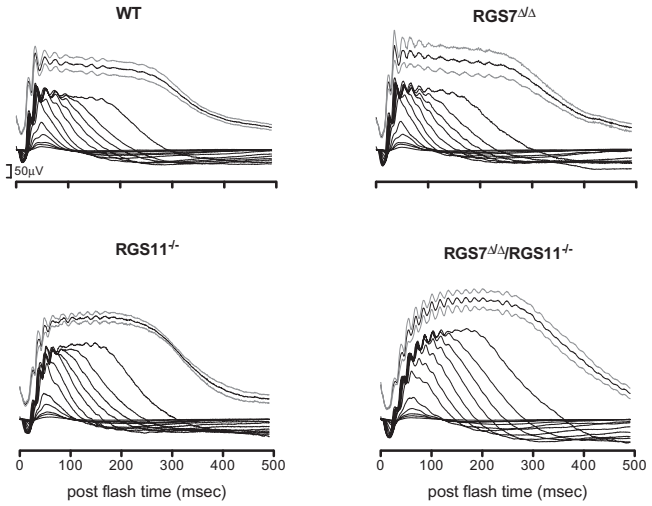

FIGURE 4. Photopic ERGs are larger in RGS11$^{-/-}$ and RGS7$^{\Delta/\Delta}$/RGS11$^{-/-}$ mice. Mean cone-mediated photopic ERGs recorded from each genotype recorded to flash intensities from −1.4 to 3.7 log phot cd-s/m^2. Mean photopic ERGs ± SE curves (*gray traces*) recorded in response to the brightest flash intensity are shown offset for each genotype. All plots are at the same scale as that shown for WT mice.

33 amino acids in the RGS7 mutant. R9AP was barely detectable in the OPL of the RGS11$^{-/-}$ and RGS7$^{\Delta/\Delta}$/RGS11$^{-/-}$ retinas, and Gβ5 immunofluorescence was reduced (Fig. 3A). A slight reduction in R9AP and Gβ5 immunofluorescence in the OPL was observed in the RGS7$^{\Delta/\Delta}$ retina. On immunoblots, the levels of R9AP and Gβ5 (both long and short forms) appeared unchanged in the mutant retinas (Fig. 3B), probably because of R9AP expression in photoreceptor outer segments[9] and Gβ5 expression in outer segments and the IPL.[21,22] The distribution and expression levels of RGS7 in the RGS11$^{-/-}$ retina and of RGS11 in the RGS7$^{\Delta/\Delta}$ retina did not appear significantly different from WT.

Photopic ERG b-Wave in the RGS11$^{-/-}$ and RGS7$^{\Delta/\Delta}$/RGS11$^{-/-}$ Mice

To investigate the effect of the deletion mutation in RGS7 and/or genetic ablation of RGS11 on the retinal light response, we compared ERGs from WT mice with those from RGS7$^{\Delta/\Delta}$, RGS11$^{-/-}$, and RGS7$^{\Delta/\Delta}$/RGS11$^{-/-}$ mice. Figure 4 shows mean cone-mediated photopic ERGs from WT and mutant mouse groups. The ERG responses from the RGS11$^{-/-}$ and RGS7$^{\Delta/\Delta}$/RGS11$^{-/-}$ mice were clearly larger and had a delayed rising phase compared with those of the WT mice. In contrast, the ERG responses of the RGS7$^{\Delta/\Delta}$ mice were indistinguishable from those of the WT mice. The key differences between the mutant and WT photopic ERGs are highlighted in Figure 5A. At the lower flash intensity (top traces), the rising phase of the photopic ERG response was markedly delayed in the RGS7$^{\Delta/\Delta}$/RGS11$^{-/-}$ mice relative to WT mice. The bottom ERG traces in Figure 5A were recorded in response to intensely bright flashes. Here, the phase of the photopic response was delayed, and the overall amplitude was larger in both the RGS11$^{-/-}$ and the RGS7$^{\Delta/\Delta}$/RGS11$^{-/-}$ mice. Maximum ERG amplitudes were obtained from filtered photopic responses after digital isolation and subtraction of the OPs (Fig. 5B, orange traces: see the Methods section). The ERG amplitude was measured at 50 and 170 ms, postflash times that correspond to the peaks of the photopic ERGs of the WT and RGS7$^{\Delta/\Delta}$/RGS11$^{-/-}$ mice, re-

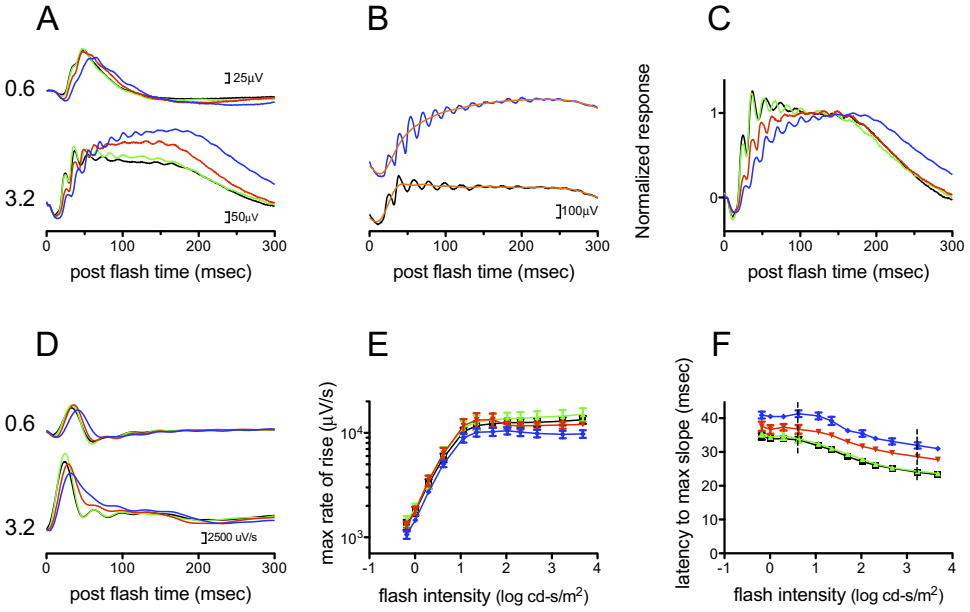

FIGURE 5. Onset of the photopic ERG is delayed in RGS11$^{-/-}$ and RGS7$^{\Delta/\Delta}$/RGS11$^{-/-}$ mice. (**A**) Mean photopic ERGs from WT (*black*), RGS7$^{\Delta/\Delta}$ (*green*), RGS11$^{-/-}$ (*red*), and RGS7$^{\Delta/\Delta}$/RGS11$^{-/-}$ (*blue*) mice are shown overlaid for two flash intensities (0.6 and 3.2 log ph cd-s/m^2). (**B**) Representative photopic ERGs from WT and RGS7$^{\Delta/\Delta}$/RGS11$^{-/-}$ mice in response to a 3.2-log phot cd-s/m^2 flash. *Orange traces*: photopic ERG responses after digital isolation and subtraction of the oscillatory potentials. (**C**) Photopic ERGs to the 3.2 log phot cd-s/m^2 flash are normalized with respect to amplitude at 170 ms, the time of peak amplitude in RGS7$^{\Delta/\Delta}$/RGS11$^{-/-}$ mice. (**D**) Means of the derivatives of the photopic ERGs for the two intensities shown. Maximum rate of increase was measured from the peak of the derivative. (**E**) Maximum rate of increase plotted as a function of flash intensity. (**F**) Latency to reach maximum rate of increase plotted as a function of flash intensity. Groups were statistically compared at the intensities indicated by the *vertical lines*. Error bars, ±SE.

TABLE 1. ERG Parameters

Parameter	WT	RGS7$^{\Delta/\Delta}$	RGS11$^{-/-}$	RGS7$^{\Delta/\Delta}$/11$^{-/-}$
ERG maximum photopic amplitudes, μV				
Measured at 50 ms	215 ± 21	205 ± 23	233 ± 20	193 ± 24
Measured at 170 ms*	181 ± 21†	159 ± 35†	281 ± 16	357 ± 38‡
Phototransduction parameters				
*R*max$_{p3}$, μV	−748 ± 42	−744 ± 71	−814 ± 48	−829 ± 45
S, (log sc cd-s/m^2)$^{-1}$ s^{-2}	3.40 ± 0.04	3.28 ± 0.04	3.49 ± 0.04	3.41 ± 0.05
td, ms	4.3 ± 0.1	4.6 ± 0.1	4.2 ± 0.2	4.5 ± 0.2
ERG b-wave parameters				
*V*max, μV	1025 ± 68	996 ± 151	1185 ± 130	1287 ± 65
K, log sc cd-s/m^2§	−2.77 ± 0.06	−2.70 ± 0.06	−2.97 ± 0.12	−2.96 ± 0.08

Data are expressed as the mean ± SE.
* One-way ANOVA: $P < 0.001$.
†‡ Columns with different symbols are significantly different at $P < 0.001$ on post hoc analysis.
§ One-way ANOVA: $P = 0.06$.

spectively. RGS7$^{\Delta/\Delta}$/RGS11$^{-/-}$ mice had significantly larger photopic ERG amplitudes at 170 ms compared with those of WT and RGS7$^{\Delta/\Delta}$ mice; there was no effect of genotype on photopic ERG amplitudes at 50 ms (Table 1).

To better compare the kinetics of the photopic ERG between mouse strains, the bright flash responses were normalized relative to amplitude at 170 ms (Fig. 5C). For WT and RGS7$^{\Delta/\Delta}$ mice, the photopic ERG rapidly rose to a peak at around 40 ms, after which the response decayed and settled at a plateau between 110 and 150 ms. In contrast, the photopic ERGs from the RGS11$^{-/-}$ and RGS7$^{\Delta/\Delta}$/RGS11$^{-/-}$ mice rose slowly to reach plateaus at 115 and 170 ms, respectively. The rates of recovery of the photopic ERG were essentially identical across all groups of mice, although the onset of this recovery was delayed in the RGS7$^{\Delta/\Delta}$/RGS11$^{-/-}$ mice (Fig. 5C).

The results in Figures 5A and 5C indicate that the rising phase of the photopic ERG response was delayed by RGS11 deficiency, a deficit that was accentuated by the addition of the RGS7 mutation. It is unclear from Figure 5A whether the ERG changes in the RGS11$^{-/-}$ and RGS7$^{\Delta/\Delta}$/RGS11$^{-/-}$ mice resulted from a decrease in the slope of the rising phase and/or a delay in the onset of the rising phase of the ERG. To investigate, we calculated the maximum rate of increase (i.e., maximum slope) of the photopic ERG from the derivative of the filtered response (see the Methods section). Figure 5D shows mean ERG derivatives for two flash intensities. The peak of the derivative function defines the maximum slope of the rising phase of the ERG response. Overall, maximum slopes were not significantly different between the ERGs of the WT and mutant mice (Fig 5E). Figure 5F shows the latency to reach the maximum slope plotted as a function of flash intensity. Responses of both the RGS11$^{-/-}$ and RGS7$^{\Delta/\Delta}$/RGS11$^{-/-}$ mice were clearly delayed relative to those of the WT and RGS7$^{\Delta/\Delta}$ mice. The magnitudes of the delays were relatively constant across flash intensities with the RGS11$^{-/-}$ responses delayed on average (±SE) by 4.0 ± 0.2 ms and the RGS7$^{\Delta/\Delta}$/RGS11$^{-/-}$ responses by 7.7 ± 0.2 ms relative to those of WT mice. Groups were statistically compared at the intensities indicated by the vertical lines in Figure 5F. The RGS11$^{-/-}$ and RGS7$^{\Delta/\Delta}$/RGS11$^{-/-}$ responses were significantly delayed ($P < 0.001$) relative to the WT and RGS7$^{\Delta/\Delta}$ responses. At the higher intensity, the RGS7$^{\Delta/\Delta}$/RGS11$^{-/-}$ responses were also significantly delayed ($P < 0.05$) relative to the RGS11$^{-/-}$ responses, demonstrating that RGS7 contributes to the ON-BPC response. The results from Figures 5C–F suggest that the delayed rising phase of the photopic ERGs in RGS11$^{-/-}$ and RGS7$^{\Delta/\Delta}$/RGS11$^{-/-}$ mice is primarily due to an increased latency before the onset of the response.

Delay of the Scotopic ERG b-Wave in the RGS11$^{-/-}$ and RGS7$^{\Delta/\Delta}$/RGS11$^{-/-}$ Mice

We also compared scotopic rod-isolated ERGs from the WT mice with those from the RGS7$^{\Delta/\Delta}$, RGS11$^{-/-}$ and RGS7$^{\Delta/\Delta}$/

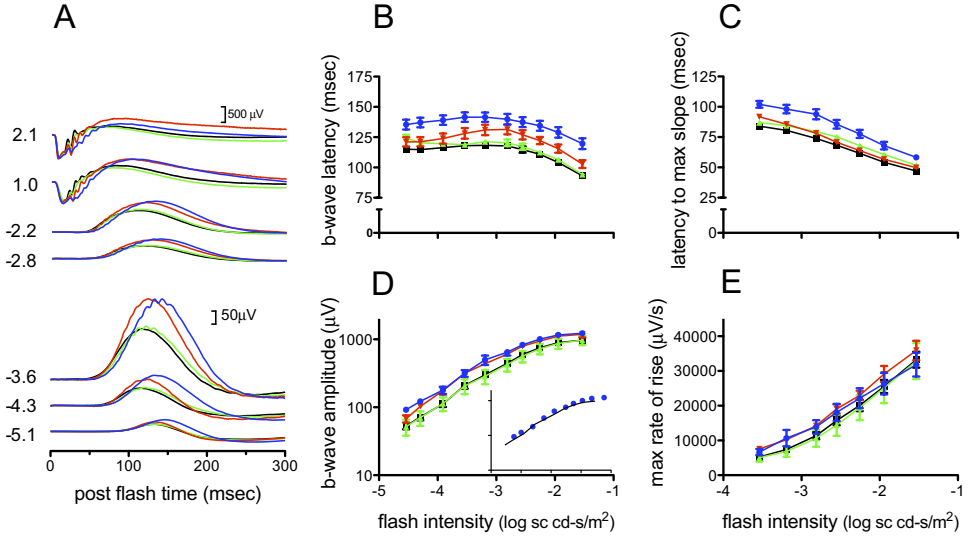

FIGURE 6. The scotopic ERG b-wave is delayed in RGS11$^{-/-}$ and RGS7$^{\Delta/\Delta}$/RGS11$^{-/-}$ mice. (**A**) Mean scotopic rod-isolated ERGs from WT (*black*), RGS7$^{\Delta/\Delta}$ (*green*), RGS11$^{-/-}$ (*red*), and RGS7$^{\Delta/\Delta}$/RGS11$^{-/-}$ (*blue*) mice. Numbers to the *left* of traces indicate flash intensity (log scot cd-s/m^2). (**B**) ERG b-wave latency plotted against flash intensity. (**C**) Latency to reach maximum rate of increase (max slope) of filtered ERG b-wave. (**D**) Maximum b-wave amplitude. *Inset*: Plot of RGS7$^{\Delta/\Delta}$/RGS11$^{-/-}$ b-wave amplitudes shifted 0.2 log unit to the right along the *x*-axis (*blue circles*). WT b-wave amplitude plots from main graph are shown with *solid black lines*. (**E**) Maximum rate of increase of filtered ERG b-wave. Error bars, ±SE.

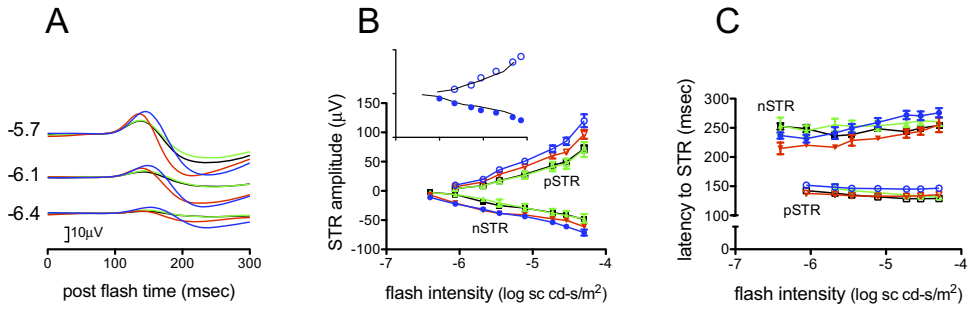

FIGURE 7. Altered STR sensitivity in RGS7$^{\Delta/\Delta}$/RGS11$^{-/-}$ mice. (**A**) Mean STRs recorded to dim flashes from WT (*black*), RGS7$^{\Delta/\Delta}$ (*green*), RGS11$^{-/-}$ (*red*), and RGS7$^{\Delta/\Delta}$/RGS11$^{-/-}$ (*blue*) mice. Numbers to the *left* of traces indicate flash intensity (log scot cd-s/m^2). (**B**) nSTR and pSTR amplitude plotted as a function of flash intensity. *Inset*: plot of RGS7$^{\Delta/\Delta}$/RGS11$^{-/-}$ nSTR and pSTR amplitudes shifted 0.4 log unit to the right along the *x*-axis (*blue circles*). *Solid black lines*: WT nSTR and pSTR amplitude plots from the main graph. (**C**) Latencies to the peaks of nSTR and pSTR. Error bars, ±SE.

RGS11$^{-/-}$ mice. Figure 6A shows mean dark-adapted rod-isolated ERGs for a range of flash intensities. Similar to our findings for the photopic ERG, the ERG b-waves from the RGS11$^{-/-}$ and RGS7$^{\Delta/\Delta}$/RGS11$^{-/-}$ mice were qualitatively larger and slower than those in the WT and RGS7$^{\Delta/\Delta}$ mice. Figure 6B clearly shows the delay to the peak of the b-waves in the RGS11$^{-/-}$ and RGS7$^{\Delta/\Delta}$/RGS11$^{-/-}$ mice. The magnitudes of the delays were relatively constant, with the responses of the RGS11$^{-/-}$ mice delayed on average (±SE) by 11.6 ± 0.5 ms and those of the RGS7$^{\Delta/\Delta}$/RGS11$^{-/-}$ mice by 24.5 ± 0.9 ms, relative to the WT mice. Statistical analysis for the highest flash intensity in Figure 6B confirmed that the b-wave peak in the RGS7$^{\Delta/\Delta}$/RGS11$^{-/-}$ mice was significantly delayed relative to that in the WT and RGS7$^{\Delta/\Delta}$ mice ($P < 0.001$) and the RGS11$^{-/-}$ mice ($P < 0.05$). While the RGS11$^{-/-}$ response appeared delayed relative to the WT and RGS7$^{\Delta/\Delta}$ responses, these delays were not significant on post hoc comparison.

There was a trend for larger b-wave amplitudes in the RGS11$^{-/-}$ and RGS7$^{\Delta/\Delta}$/RGS11$^{-/-}$ mice (Fig 6D) although differences in maximum b-wave amplitude were not significant (Table 1). In contrast, there was a borderline significant difference ($P < 0.06$) in rod b-wave sensitivity, with the RGS11$^{-/-}$ and RGS7$^{\Delta/\Delta}$/RGS11$^{-/-}$ mice some 0.2 log units more sensitive than the WT and RGS7$^{\Delta/\Delta}$ mice (K, Table 1). As for the photopic responses, to examine whether the delayed b-wave resulted from a reduced slope or slower onset of the response, we calculated the maximum slope of the filtered scotopic b-wave. There was no difference in the maximum b-wave slope between the mice (Fig 6E), and the delay in latency to reach the maximum slope in the RGS7$^{\Delta/\Delta}$/RGS11$^{-/-}$ mice (Fig 6C) was consistent with the delay to the peak of the b-wave. Together these results suggest a slightly increased scotopic b-wave sensitivity in RGS11$^{-/-}$ and RGS7$^{\Delta/\Delta}$/RGS11$^{-/-}$ mice and indicate that a delay in the onset of the b-wave accounts for the delayed b-wave peak. Phototransduction parameters were not different between genotypes (Table 1), indicating that the delays in the scotopic ERGs resulted from changes downstream of the photoreceptors.

Enhanced Scotopic Threshold Sensitivity in the RGS11$^{-/-}$ and RGS7$^{\Delta/\Delta}$/RGS11$^{-/-}$ Mice

We also examined the effects of the RGS7 and -11 mutations on the scotopic threshold response (STR). Figure 7A shows STRs illustrating both the positive (p)STR and negative (n)STR components. These STR components originate within the proximal retina, most likely from the amacrine and ganglion cells in mice.[38] In Figures 7B and 7C the amplitudes and latencies of the two STR components are plotted as functions of flash intensity. As for the ERG b-wave, the RGS11$^{-/-}$ and RGS7$^{\Delta/\Delta}$/RGS11$^{-/-}$ mice had greater STR sensitivity. The inset in Figure 7B demonstrates this increase in sensitivity. Here, the STR amplitude plots of the RGS7$^{\Delta/\Delta}$/RGS11$^{-/-}$ mice (blue symbols) have been shifted 0.4 log units right along the *x*-axis where they almost perfectly overlap the STR amplitude plots from the WT mice (solid lines). The times to reach the peaks of the STR components were not different between the WT and mutant mice (Fig 7C). These results indicate a slightly larger increase in STR sensitivity in the RGS11$^{-/-}$ and RGS7$^{\Delta/\Delta}$/RGS11$^{-/-}$ mice than would be predicted from the b-wave results, possibly resulting from more sustained output from the bipolar cells into the proximal retina.

Effect of RGS7 and -11 on Simulated Light Responses from Individual Rod BPCs

To investigate the combined effect of genetic ablation of RGS11 and the deletion mutation in RGS7 on the kinetics of the ON-BPC light response, we compared chemically simulated light responses from rod BPCs in retinal slices from WT and RGS7$^{\Delta/\Delta}$/RGS11$^{-/-}$ mice. This technique allowed us to bypass the photoreceptors entirely, thereby eliminating any effect of impaired signaling in these cells in the RGS7$^{\Delta/\Delta}$/RGS11$^{-/-}$ retina. In some experiments, rod bipolar cells were morphologically identified by filling with Alexa-488 hydrazide during whole-cell recording; in other instances, rod BPCs were identified by their characteristic peak-to-plateau response, which is readily distinguishable from the more sustained response in cone ON-bipolar cells.[5] As shown in Figure 8, the CPPG responses of the rod BPCs were similar in overall shape, indicat-

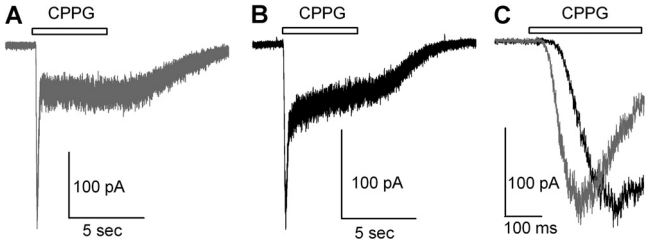

FIGURE 8. Simulated light responses from rod BPCs in the WT and RGS7$^{\Delta/\Delta}$/RGS11$^{-/-}$ retinas. The CPPG responses of cells from the WT (**A**) and RGS7$^{\Delta/\Delta}$/RGS11$^{-/-}$ (**B**) mice were grossly similar. The time-course of the response is compared by showing normalized responses on an expanded timescale (**C**). As shown, the onset of the CPPG response was delayed by ~25 ms in rod BPCs in the RGS7$^{\Delta/\Delta}$RGS11$^{-/-}$ retina.

Table 2. ON-BPC Electrophysiological Responses

	WT (n = 72)	RGS7$^{\Delta/\Delta}$/11$^{-/-}$ (n = 44)
Response amplitude, pA	146 ± 7	148 ± 6
10%–90% rise, ms	84 ± 5	90 ± 4
Delay, ms	50 ± 2	74 ± 3

Data are expressed as the mean ± SE.

ing that rod BPC function was not grossly disrupted in the RGS7$^{\Delta/\Delta}$/RGS11$^{-/-}$ retina; however, the onset of the response in the RGS7$^{\Delta/\Delta}$/RGS11$^{-/-}$ retina was delayed by ~25 ms (Fig. 8C). As determined by the time interval from pressure application to the 10% increase time, the delay in the onset of the CPPG response increased from 50.3 ± 1.8 to 74 ± 3.1 ms ($P <$ 0.001; SEM). In contrast, the amplitude and 10% to 90% increase times were unaffected (Table 2). We also recorded simulated light responses from rod BPCs in retinal slices from the RGS7$^{\Delta/\Delta}$ and RGS11$^{-/-}$ mice. There was no detectable delay in the response from RGS7$^{\Delta/\Delta}$ mice (n = 8). The responses from the RGS11$^{-/-}$ cells were delayed slightly (~10 ms) but this result was not statistically significant given the relatively small number of recordings (n = 15). Nevertheless, the above results strongly suggest that RGS7 and/or -11 play a role in the deactivation of Gαo, which precedes activation of the depolarizing current in these cells.

Discussion

Deactivation of the mGluR6-Go signaling cascade underlies the light response of retinal ON-BPCs. We confirmed that GTP hydrolysis is essential for deactivation of the pathway, yet the intrinsic GTPase rate of Gαo is too slow[7,8] to account for the rapid kinetics of this response. In the past decade, RGS protein complexes have been shown to accelerate GTP hydrolysis and promote rapid termination of many cellular responses. In retinal photoreceptors, the RGS9-Gβ5-R9AP complex stimulates GTP hydrolysis by GαT, thereby accelerating recovery of the photoresponse.[11] Recently, our laboratories and others have demonstrated that similar complexes containing RGS7 and -11 are present in the dendritic tips of ON-BPCs, suggesting a role for these proteins in the mGluR6 signal transduction pathway.[21–24] Here, we present evidence that RGS7 and -11 play a role in regulating the onset, amplitude, and sensitivity of the ON-BPC light response.

Genetic deletion of RGS11 leads to striking effects on the levels of its binding partners. Immunoblots from RGS11$^{-/-}$ retina reveal a dramatic reduction of R9AP and Gβ5 protein levels in the OPL (Fig. 2). Similar results were recently reported by Cao et al.[23] A reduction of Gβ5 is also seen in photoreceptors of RGS9$^{-/-}$ mice.[10] In photoreceptors, proper formation of the entire RGS9-Gβ5-R9AP complex is necessary to prevent rapid proteolytic degradation of the individual protein components,[10,12] and this appears to be the case for the RGS11 complex in ON-BPC dendrites.

The delay in the onset of the rising phase of both the rod- and cone-isolated ERG b-waves and the chemically simulated rod BPC light response in the RGS11$^{-/-}$ and RGS7$^{\Delta/\Delta}$/RGS11$^{-/-}$ mice suggests a role for RGS11-Gβ5-R9AP in accelerating an early phase of Go inactivation. Mojumder et al.[24] similarly reported delays in ERGs from RGS11- and RGS7-deficient mice. We found no change in the maximum rates of increase of the ERG b-wave across genotype, suggesting that RGS11-Gβ5-R9AP is not absolutely necessary for ON-BPC responses. We also found much larger photopic ERG amplitudes in RGS11$^{-/-}$ and RGS7$^{\Delta/\Delta}$/RGS11$^{-/-}$ mice at longer poststimulus times. The bright flash and photopic ERGs from these mice lacked the initial overshoot seen in the WT RGS7$^{\Delta/\Delta}$ mice (Fig. 5C), and instead continued to increase over a longer period, which generated the larger amplitudes. However, the mechanism underlying the increased photopic amplitudes remains to be elucidated. Larger photopic amplitudes were not reported for RGS11$^{-/-}$ mice by Mojumder et al.,[24] but we used a brighter flash (>400-fold), which may account for the difference in results.

The increase in STR sensitivity in the RGS11$^{-/-}$ and RGS7$^{\Delta/\Delta}$/RGS11$^{-/-}$ mice was slightly greater than for the b-wave, suggesting that the change in the ON-BPC light response of these mice is propagated downstream to amacrine and ganglion cells. Our STR results are in contrast to those of Mojumder et al.[24] who reported attenuated STRs from RGS7- and RGS11-deficient mice. The cause of the difference in STR results could be due to differences in experimental techniques used to record the STR (e.g., reference electrode location), but this remains to be determined.

Unlike RGS11, the deletion mutation of RGS7 had little effect on the distribution of RGS11, Gβ5, or R9AP, and had no discernable effect on the ERG. It is clear, however, that RGS7 plays a role in the ON-BPC response, as the delay in the onset of both the rod and cone-isolated ERG b-waves and in the increase of the chemically simulated rod BPC light response were accentuated in RGS7$^{\Delta/\Delta}$/RGS11$^{-/-}$ mice compared with those of the RGS11$^{-/-}$ mice. Furthermore, Mojumder et al.[24] reported a small delay in the rising phase of the scotopic b-wave in the RGS7 mutant. Compared with the other three mouse groups, we had higher variability in the ERG measurements from our RGS7$^{\Delta/\Delta}$ mice, which may have masked the subtle scotopic ERG changes reported in these mice by Mojumder et al.[24] However, these findings suggest that, although the RGS7 mutant is functionally impaired, these mice probably retain GTPase accelerating activity. It is possible that RGS7 and -11 serve redundant functions in the ON-BPC dendrites and that RGS7, and even RGS7$^{\Delta/\Delta}$, can compensate for loss of RGS11 in the RGS11$^{-/-}$ retina. Generation of true RGS7/11 double knockouts is likely to be necessary to reveal the full extent of the effect of R7 RGS proteins on the ON-BPC light response.

Acknowledgments

The authors thank Shixi Zheng, Celia Gellman, and Jacqueline Gayet for assistance with immunohistochemistry and genotyping and Theodore G. Wensel for reagents, discussions, and encouragement.

References

1. Nakajima Y, Iwakabe H, Akazawa C, et al. Molecular characterization of a novel retinal metabotropic glutamate receptor mGluR6 with a high agonist selectivity for L-2-amino-4-phosphonobutyrate. *J Biol Chem.* 1993;268:11868–11873.
2. Vardi N. Alpha subunit of Go localizes in the dendritic tips of ON bipolar cells. *J Comp Neurol.* 1998;395:43–52.
3. Nawy S. The metabotropic receptor mGluR6 may signal through G (o), but not phosphodiesterase, in retinal bipolar cells. *J Neurosci*. 1999;19:2938–2944.
4. Morgans CW, Zhang J, Jeffrey BG, et al. TRPM1 is required for the depolarizing light response in retinal ON-bipolar cell. *Proc. Natl Acad Sci U S A.* 2009;106:19174–19178.
5. Berntson A, Taylor WR. Response characteristics and receptive field widths of on-bipolar cells in the mouse retina. *J Physiol.* 2000;524:879–889.
6. Xie GX, Palmer PP. How regulators of G protein signaling achieve selective regulation. *J Mol Biol.* 2007;366:349–365.
7. Higashijima T, Ferguson KM, Smigel MD, Gilman AG. The effect of GTP and Mg2+ on the GTPase activity and the fluorescent properties of Go. *J Biol Chem.* 1987;262:757–761.

8. Lan KL, Remmers AE, Neubig RR. Roles of G (o) alpha tryptophans in GTP hydrolysis, GDP release, and fluorescence signals. *Biochemistry.* 1998;37:837–843.
9. Hu G, Wensel TG. R9AP, a membrane anchor for the photoreceptor GTPase accelerating protein, RGS9–1. *Proc Natl Acad Sci U S A.* 2002;99:9755–9760.
10. Chen CK, Burns ME, He W, Wensel TG, Baylor DA, Simon MI. Slowed recovery of rod photoresponse in mice lacking the GTPase accelerating protein RGS9–1. *Nature.* 2000;403:557–560.
11. Krispel CM, Chen CK, Simon MI, Burns ME. Prolonged photoresponses and defective adaptation in rods of Gbeta5−/− mice. *J Neurosci.* 2003;23:6965–6971.
12. Keresztes G, Martemyanov KA, Krispel CM, et al. Absence of the RGS9-Gbeta5 GTPase-activating complex in photoreceptors of the R9AP knockout mouse. *J Biol Chem.* 2004;279:1581–1584.
13. Willars GB. Mammalian RGS proteins: multifunctional regulators of cellular signalling. *Semin Cell Dev Biol.* 2006;17:363–376.
14. Popov S, Yu K, Kozasa T, Wilkie TM. The regulators of G protein signaling (RGS) domains of RGS4, RGS10, and GAIP retain GTPase activating protein activity in vitro. *Proc Natl Acad Sci U S A.* 1997;94:7216–7220.
15. Hooks SB, Harden TK. Purification and in vitro functional analysis of R7 subfamily RGS proteins in complex with Gbeta5. *Methods Enzymol.* 2004;390:163–177.
16. Kovoor A, Seyffarth P, Ebert J, et al. D2 dopamine receptors co-localize regulator of G-protein signaling 9–2 (RGS9–2) via the RGS9 DEP domain, and RGS9 knock-out mice develop dyskinesias associated with dopamine pathways. *J Neurosci.* 2005;25:2157–2165.
17. Hu G, Zhang Z, Wensel TG. Activation of RGS9–1GTPase acceleration by its membrane anchor, R9AP. *J Biol Chem.* 2003;278:14550–14554.
18. Drenan RM, Doupnik CA, Boyle MP, et al. Palmitoylation regulates plasma membrane-nuclear shuttling of R7BP, a novel membrane anchor for the RGS7 family. *J Cell Biol.* 2005;169:623–633.
19. Martemyanov KA, Yoo PJ, Skiba NP, Arshavsky VY. R7BP, a novel neuronal protein interacting with RGS proteins of the R7 family. *J Biol Chem.* 2005;280:5133–5136.
20. Song JH, Song H, Wensel TG, Sokolov M, Martemyanov KA. Localization and differential interaction of R7 RGS proteins with their membrane anchors R7BP and R9AP in neurons of vertebrate retina. *Mol Cell Neurosci.* 2007;35:311–319.
21. Morgans CW, Weiwei Liu, Wensel TG, et al. Gbeta5-RGS complexes co-localize with mGluR6 in retinal ON-bipolar cells. *Eur J Neurosci.* 2007;26:2899–2905.
22. Rao A, Dallman R, Henderson S, Chen CK. Gbeta5 is required for normal light responses and morphology of retinal ON-bipolar cells. *J Neurosci.* 2007;27:14199–14204.
23. Cao Y, Masuho I, Okawa H, et al. Retina-specific GTPase accelerator RGS11/G beta 5S/R9AP is a constitutive heterotrimer selectively targeted to mGluR6 in ON-bipolar neurons. *J Neurosci.* 2009;29:9301–9313.
24. Mojumder DK, Qian Y, Wensel TG. Two R7 regulator of G-protein signaling proteins shape retinal bipolar cell signaling. *J Neurosci.* 2009;29:7753–7765.
25. Cheever ML, Snyder JT, Gershburg S, Siderovski DP, Harden TK, Sondek J. Crystal structure of the multifunctional Gbeta5-RGS9 complex. *Nat Struct Mol Biol.* 2008;15:155–162.
26. Berntson A, Taylor WR, Morgans CW. Molecular identity, synaptic localization, and physiology of calcium channels in retinal bipolar cells. *J Neurosci Res.* 2003;71:146–151.
27. Morgans CW, Bayley PR, Oesch NW, Ren G, Akileswaran L, Taylor WR. Photoreceptor calcium channels: insight from night blindness. *Vis Neurosci.* 2005;22:561–568.
28. Chen CK, Eversole-Cire P, Zhang H, et al. Instability of GGL domain-containing RGS proteins in mice lacking the G protein beta-subunit Gbeta5. *Proc Natl Acad Sci U S A.* 2003;100:6604–6609.
29. Morgans CW, Ren G, Akileswaran L. Localization of nyctalopin in the mammalian retina. *Eur J Neurosci.* 2006;23:1163–1171.
30. Dodt HU, Eder M, Schierloh A, Zieglgänsberger W. Infrared-guided laser stimulation of neurons in brain slices. *Sci STKE.* 2002;2002:PL2.
31. Wyszecki G, Stiles WS. *Color Science*: *Concepts and Methods*, *Quantitative Data and Formulae*. New York: John Wiley & Sons; 1982.
32. Birch DG, Hood DC, Nusinowitz S, Pepperberg DR. Abnormal activation and inactivation mechanisms of rod transduction in patients with autosomal dominant retinitis pigmentosa and the pro-23-his mutation. *Invest Ophthalmol Vis Sci.* 1995;36:1603–1614.
33. Pennesi ME, Howes KA, Baehr W, Wu SM. Guanylate cyclase-activating protein (GCAP) 1 rescues cone recovery kinetics in GCAP1/GCAP2 knockout mice. *Proc Natl Acad Sci U S A.* 2003;100:6783–6788.
34. Fulton AB, Rushton WA. The human rod ERG: correlation with psychophysical responses in light and dark adaptation. *Vision Res.* 1978;18:793–800.
35. Nawy S. Regulation of the on bipolar cell mGluR6 pathway by Ca2+. *J Neurosci.* 2000;20:4471–4479.
36. Nawy S, Jahr CE. cGMP-gated conductance in retinal bipolar cells is suppressed by the photoreceptor transmitter. *Neuron.* 1991;7:677–683.
37. Sampath AP, Rieke F. Selective transmission of single photon responses by saturation at the rod-to-rod bipolar synapse. *Neuron.* 2004;41:431–443.
38. Saszik SM, Robson JG, Frishman LJ. The scotopic threshold response of the dark-adapted electroretinogram of the mouse. *J Physiol.* 2002;543:899–916.